Novel N,O-Containing Microporous Carbon Frameworks as Electrode for Supercapacitors

Fangyuan HU(胡方圆),[a] Jinyan WANG(王锦艳),[a] Shui HU,[a] Linfei LI,[a] Xigao JIAN (蹇锡高)[a*]

Abstract: The N,O-containing micropore-dominated materials are developed successfully via temperature-dependent cross-linking of 4,4'-(dioxo-diphenyl-2,3,6,7-tetraaza-anthracene-diyl)-dibenzonitrile (DPDN) monomers. By employing the molecular engineering strategy, we have designed and synthesized a series of porous heteroatoms-containing carbon frameworks (PHCFs) in which the nitrogen and oxygen heteroatoms distribute homogeneously through the whole framework at atomic level, which can ensure the stability of the electrical properties. The as-made PHCFs@550 exhibits a high specific capacitance of 378 F g^{-1}, with an excellent long cycle life, whereby excellent cycle stability (ca. 120 % capacitance retention for 20000 cycles). Moreover, the successful preparation of PHCFs provides new insights for the fabrication of the nitrogen and oxygen containing electrode materials from readily available components through a facile routine.

1. Introduction

Supercapacitors have become a novel energy storage device due to its outstanding advantages with high power density and long cycle life.[1] Carbonaceous materials have been widely used as the electrode materials for supercapacitors[2] due to their abundant sources, large specific surface area, varieties of forms and high conductivity. Carbon-based supercapacitors hold excellent power density and good reversibility as well as low cost.[3] Nevertheless, the low energy density of traditional carbon-based supercapacitors (mostly less than 6 Wh/kg in commercially available supercapacitors) has significantly limited their widespread application in primary power sources.[4]

It is well known that the energy density (E) of supercapacitors mainly depends on the specific capacitance (C) and operational voltage (V) based on the equation $E=1/2(CV^2)$.[4] Thus, significant research has been directed toward improving their energy density by (1) increasing the specific capacitance (C) with high surface area carbon electrode materials and (2) enhancing the operational voltage (V) with electrolytes that possess high potential windows.[5] These two parameters are determined mainly by electrodes, therefore, previous attempts at increasing the specific capacitance (C) of supercapacitors have dealt extensively via rational design of various electrode materials, such as the development of new carbonaceous materials,[6] the increase of the effective surface area,[7] the adjustment of pore size distribution,[8] and the introduction of heteroatoms into the carbon skeletons, including nitrogen, oxygen, phosphorus, sulfur and boron. Among these existing approaches, the introduction of heteroatoms into the electrode materials is attracting considerable attention since it not only enables the enhancement of conductivity, wettability and electro-active surface area of the electrode, but also endows the electrode with pseudocapacitance (fast redox reaction between the electrolyte and the electroactive species on the electrode surface),[9] thus, further improves their electrochemical performance. However, traditional heteroatoms doped in various carbonaceous materials, such as heteroatoms doped in reduced graphene oxide, carbon nanotubes, mesoporous carbons, etc., usually exhibit random structures with high uncertainty, resulting in unstable performance in use. Consequently, carbonaceous materials with more accurate structures are desired to explore dramatically. So far, heteroatoms can be introduced into the frameworks with defined pore

sizes controllably by ionothermal synthesis. Another effective solution to improve the specific capacity (C) is to create micropores. Many research works including theoretical calculations and experimental results have revealed that micropores in the electrode can contribute significantly to the capacitance. Unfortunately, common physical or chemical activation methods always produce a wide range of pore size distribution, ranging from micro-size to macro-size. Therefore, novel preparation methods providing a controllable pore structure are necessary for further development of supercapacitive electrodes. Meanwhile, the rational design of supercapacitive electrodes to meet large capacitance, high energy density and outstanding stability, remains a substantial challenge.
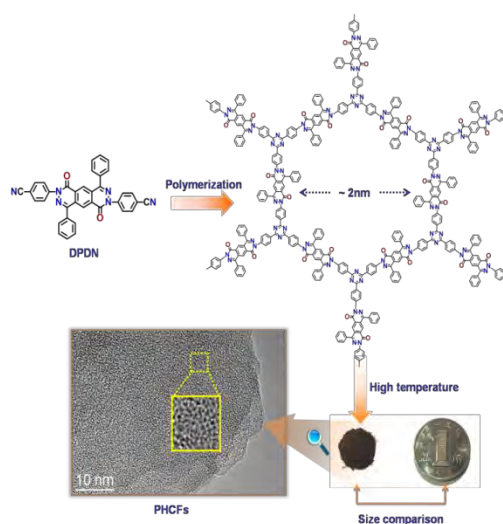
Scheme 1 Illustration of the preparation of PHCFs, including the polymerization of DPDN and high-temperature to form nitrogen and oxygen contained microporous framework of PHCFs.

Based on the considerations mentioned above, nitrogen and oxygen both in carbon frameworks are successfully developed via temperature-dependent cross-linking of a monomer containing nitrogen and oxygen heteroatoms, 4,4'-(1,6-dioxo-4,9-diphenylpyridazino[4,5-g]phthalazine-2,7(1H,6H)-diyl)di-benzonitrile (DPDN), as the basic building block. DPDNs experience the trimerization of cyano groups, and subsequent ionothermal synthesis to build a microporous structure with enhanced conductivity (Scheme 1). To the best of our knowledge, this is the first time that these porous heteroatoms-containing carbon frameworks (PHCFs) analogues are engineered into electrode materials in supercapacitors. In the frameworks containing nitrogen and oxygen heteroatoms, nitrogen-containing generally provides basic characteristics, and the oxygen-containing could have an acidic character, behaving as electron acceptors, inducing electron-donor properties.[47] Eventually, a novel electrode material for supercapacitors with high capacitance (*i.e.*, 378 F g^{-1} at 0.1 A g^{-1}) is obtained without sacrificing high cycling stability (ca. 120 % capacitance retention for 20000 cycles).

2. Results and discussion

As a representative example, it is found that the PHCFs@600 is composed of extremely abundant uniform porous frameworks as revealed by the HR-TEM image (Fig. 1a), and its elemental mapping images on carbon, nitrogen and oxygen further demonstrate the homogeneous distribution of carbon, nitrogen and oxygen in the skeletons of PHCFs@600 (Fig. 1b-1d). Moreover, quantitative analyses of nitrogen and oxygen atoms based on the elemental analyses and the XPS characterizations (Fig. 1e), respectively, show that both the

nitrogen and oxygen contents in PHCFs drop rapidly with the increase of the polymerization temperatures, which indicates that the polymerization temperature greatly affects the composition and thus the chemical structure of PHCFs.
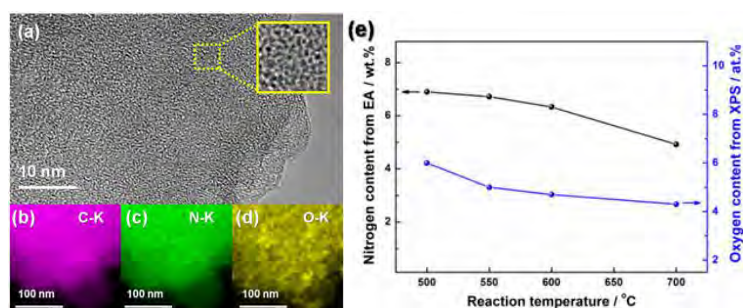

Fig. 1 (a) High resolution transmission electron microscopy (HR-TEM) image of PHCFs@600; (b) Carbon atom mapping image of PHCFs@600; (c) Nitrogen atom mapping image of PHCFs@600; (d) Oxygen atom mapping image of PHCFs@600; (e) Nitrogen and oxygen contents of PHCFs prepared at different temperatures from EA (wt. %) and XPS (at. %), respectively.

The pore structures of PHCFs are also evaluated by the nitrogen adsorption/desorption measurement at 77 K. The result reveals that PHCFs are microporous and exhibits typical type I reversible sorption profiles (Fig. 2a). Evaluation of the pore size distribution based on the density functional theory (DFT) further verifies this finding (Fig. 2b). Additionally, the maximum of the Brunauer-Emmett-Teller (BET) surface areas of PHCFs is 1244 m^2/g when the polymerization temperatures is 550 ^oC.
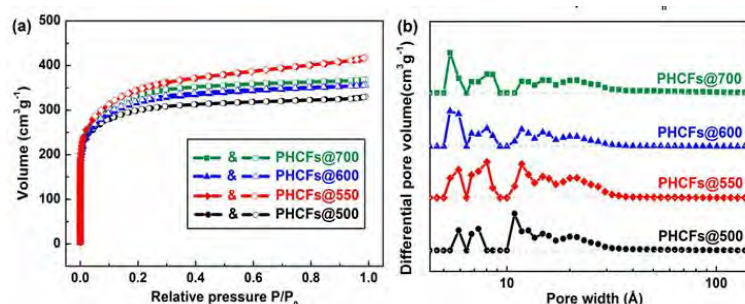

Fig.2 (a) Nitrogen adsorption/desorption isotherms of PHCFs; (b) pore size distributions of PHCFs.

To evaluate the supercapacitive performances of PHCFs, cyclic voltammetry (CV), galvanostatic charge-discharge (GC) and electrochemical impedance spectroscopy (EIS) are examined in 1 M H_2SO_4 aqueous electrolyte in a conventional three-electrode system. Cyclic voltammetry (CV) curves for PHCFs@600 at different scan rates are shown in Fig. 3a. Obviously, PHCFs@600 exhibits symmetric *I-V* curves and affords reversible voltage-dependent current loops which is typical of the supercapacitive energy storage. Fig. 3b shows the typical charge-discharge curves of PHCFs@600 electrode at different current densities. It is obvious that the charge and discharge curves show nearly triangular shapes when the polymerization temperature is 550 ^oC or higher. Among them, the PHCFs@550 electrode displays the highest specific capacitance of 378 F g^{-1} at a current density of 0.1 A g^{-1}, which is well consistent with the above CV results. It also suggests that the fast ion transport and quick electron propagation occurs within PHCFs@550 electrode. The specific capacitance

values of PHCFs are summarized in Fig. 3c. It reveals that the electrochemical performance is closely related to the polymerization temperature. When the polymerization temperature increases, the specific capacitance at a current density of 0.1 A g^{-1} first increases from 175 F g^{-1} (PHCFs@500), 378 F g^{-1} (PHCFs@550), then decreases to 264 F g^{-1} (PHCFs@600), 230 F g^{-1} (PHCFs@700). Furthermore, Fig. 3c also shows that the specific capacitance values of both PHCFs@500 and PHCFs@550 decrease much quicker than other PHCFs as the current density increases, which may be associated with their lower polymerization temperature. Supercapacitor performance is further analyzed using electrochemical impedance spectroscopy (EIS) technique to correlate electrolyte ion transport limitations with microstructures of PHCFs electrodes (shown as Fig. 3d). The resistance of the PHCFs electrodes highly depends on the polymerization temperature. The nearly vertical line in the low frequency region shows that the PHCFs@700 electrode has outstanding ion diffusion and migration behavior compared with the other PHCFs, exhibiting the best capacitive behavior.

In addition, the excellent capacitance retention is promising for application in which a high rate of discharge-recharge is required. Thus, the cycling stability of the PHCFs@550 electrode has been tested by the galvanostatic charge-discharge measurement at a current density of 5.0 A g^{-1} (shown as Fig. 4a). Notably, its specific capacitance shows a tendency of rise instead of decline after 20000 cycles in 1M H_2SO_4, indicating a long-term stability of the electrode. It could be possibly attributed to the improved wettability and active process of the electrode (PHCFs@550). These changes allow the trapped electrolyte ions diffuse out. Meanwhile, the charge-discharge curves maintain triangular even after 20000 cycles (shown as the inset of Fig. 4a). The above results indicate that our electrode has excellent electrical cycling stability.
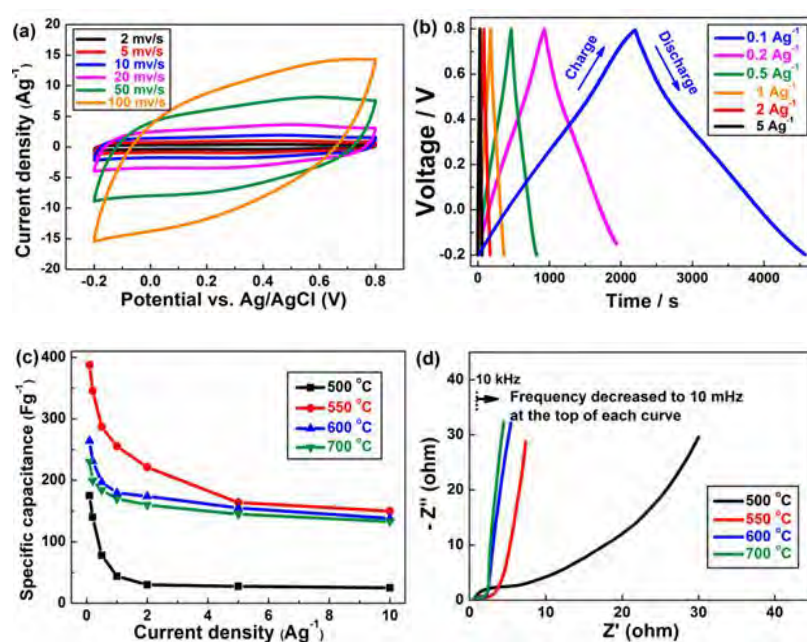

Fig. 3 (a) Cyclic voltammograms of PHCFs@600 electrodes measured in a three-electrode system at different scan rates; (b) Charge-discharge curves of PHCFs@600 electrodes at different current densities; (c) Specific capacitances at various current densities; (d) Nyquist plots (AC frequency ranges from 10 kHz to 10 MHz) of PHCFs electrodes.
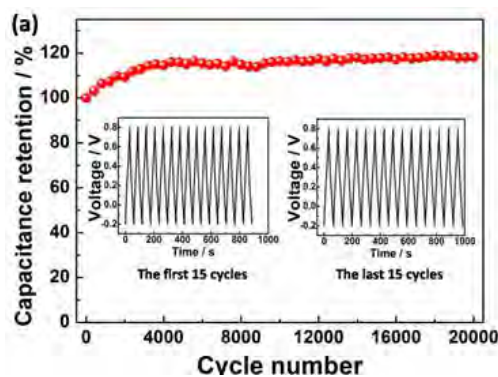
Fig. 4 (a) Cycle life tests with a three-electrode setup at 5.0 A g^{-1}. The first and last fifteen cycles of GC curves are shown in the inset; the supercapacitor can drive a commercial red LED at 2.0 V assembled in two devices: (b) assembled in PTFE mold; (c) assembled in Swagelok cell.

3. Conclusions

In summary, we demonstrate an efficient strategy of designing high-performance PHCFs electrodes based on micropore-dominanted structures with nitrogen and oxygen contained. The greatly enhanced electrochemical performance, resulting from the pseudocapacitive behavior and wettability from intrinsic heteroatoms, provides a high specific capacitance up to 378 F g^{-1}. Moreover, PHCFs@550 electrode displays exceptional cyclic stability (ca. 120 % capacitance retention for 20000 cycles). Notably, the achieved specific capacitance values are much higher than those reported under similar testing conditions for other elaborately designed carbonaceous materials such as activated carbon, carbon nanotubes, and graphene, which mark their great potential as electrode materials in supercapacitors.

Acknowledgements

Notes and references

[1] M. Winter, R. J. Brodd, *Chem. Rev.*, 2004, **104**, 4245.
[2] P. Simon, Y. Gogotsi, *Acc. Chem. Res.,* 2012, **46**, 1094.
[3] A. Ghosh, Y. H. Lee, *ChemSusChem,* 2012, **5**, 480.
[4] L. Hao, X. Li, L. Zhi. *Adv. Mater.,* 2013, **25**, 3899.
[5] L. Zhang, F. Zhang, X. Yang, K. Leng, Y. Huang, Y. Chen, *Small,* 2013, **9**, 1342.
[6] X. Yang, J. Zhu, L. Qiu, D. Li, *Adv. Mater.,* 2011, **23**, 2833.
[7] H. Nishihara, T. Kyotani, *Adv. Mater.,* 2012, **24**, 4473.
[7] M. Xue, F. Li, J. Zhu, H. Song, M. Zhang, T. Cao, *Adv. Funct. Mater*., 2012, **22**, 1284.
[8] L. Zhang, X. Yang, F. Zhang, G. Long, T. Zhang, K. Leng, Y. Zhang, Y. Huang, Y. Ma, M. Zhang, Y. Chen, *J. Am. Chem. Soc.,* 2013, **135**, 5921.